

# **Study on Curcumin based nanomedicine against Cancer Stem Cells**

*A Major Project dissertation submitted*

*in partial fulfilment of the requirement for the degree of*

**Master of Technology**

**In**

**Biomedical Engineering**

*Submitted by*

**Naina Gupta**

**(2K15/BME/04)**

**Delhi Technological University, Delhi, India**

*Under the supervision of*

**Dr. Vimal Kishor Singh**



Department of Biotechnology  
Delhi Technological University  
(Formerly Delhi College of Engineering)  
Shahbad Daultpur, Main Bawana Road,  
Delhi-110042, INDIA



## CERTIFICATE

This is to certify that the M. Tech. dissertation entitled “**Study on Curcumin based nanomedicine against Cancer Stem Cells**”, submitted by **NAINA GUPTA (2K15/BME/04)** in partial fulfilment of the requirement for the award of the degree of Master of Engineering, Delhi Technological University (Formerly Delhi College of Engineering, University of Delhi), is an authentic record of the candidate’s own work carried out by her under our guidance.

The information and data enclosed in this dissertation is original and has not been submitted elsewhere for honouring of any other degree.

**Date:**

**Dr. Vimal Kishor Singh**  
(Project Supervisor)  
Department of Biotechnology  
Delhi Technological University

**Prof D. Kumar**  
Co-supervisor  
Head of Department  
Department of Biotechnology

# ACKNOWLEDGEMENT

First and foremost, my sincere thanks to Prof. D. Kumar, Head, Department of Biotechnology, Delhi Technological University, for giving me an opportunity to study and work in this prestigious institute.

I would like to express my warm gratitude to Dr. Vimal Kishor Singh for not only giving me a platform to learn but also for his guidance, persistent encouragement and valuable suggestions throughout the project work.

I am extremely thankful to SMITA Labs, IIT Delhi and Dr. Rajesh Tandon, Department of Botany, Delhi University for allowing me to carry out my research work in their laboratory.

Next, I would like to give special thanks to Mr. Abhishek Saini and Ms. Vishwachi for their constant support and friendly advices which were extremely valuable for my study both theoretically and practically.

NAINA GUPTA

2K15/BME/04

# CONTENTS

<b>TOPIC</b>	<b>PAGE NO</b>
<i>LIST OF FIGURES</i>	5
<i>LIST OF TABLES</i>	6
<i>LIST OF ABBREVIATIONS</i>	7
<b>1. ABSTRACT</b>	9
<b>2. INTRODUCTION</b>	11
<b>3. REVIEW OF LITERATURE</b>	16
<b>4. AIM AND OBJECTIVE</b>	24
<b>5. METHODOLOGY</b>	26
<b>6. RESULTS</b>	31
<b>7. DISCUSSION</b>	48
<b>8. CONCLUSION</b>	50
<b>9. REFERENCES</b>	52

## LIST OF FIGURES

Figure no.	Figure name	Page no.
2.1	Structure of micelle	14
2.2	Chemical structure of Curcumin	15
3.1	Need for cancer stem cell specific therapy	17
3.2	Formation of micelle	22
3.3	Overview of anti cancer effects of Curcumin	23
6.1	Preparation of RPMI-1640 media	33
6.2	Subculturing of YAC-1 cell line	34
6.3	YAC-1 cells in T75 culture flask	34
6.4	Cell viability analysis using trypan blue	35
6.5	Cell morphology analysis using Giemsa stain	35
6.6	Growth curve of YAC-1 cell line	37
6.7	Dissolution of lipid in organic solvent	38
6.8	Formation of thin film after evaporation of organic solvent while preparing	38
6.9	Bath Sonicator and sonication of micelles	39
6.10	Appearance of micelles	39
6.11	Graphical Representation of Curcumin Standard Curve	40
6.12	Particle size of Curcumin micelles	41
6.13	SEM images	42
6.14	FTIR spectra of Curcumin	43
6.15	FTIR spectra of Curcumin micelles	43
6.16	Evaluation of anticancer activity in 24 wells plate	44
6.17	24 wells plate after 72 hour incubation in 5% CO <sub>2</sub> incubator	45
6.18	Cells plated into 96 wells plate for MTT assay	45
6.19	Cells treated with MTT assay after 4 hours of incubation in 5% CO <sub>2</sub> incubator	46
6.20	Graph representing cell viability by MTT assay	46

## LIST OF TABLES

Table no.	Table name	Page no.
1.	Observation Table of Growth Curve Analysis	35
2.	Observation Table of Curcumin standard curve	39

# LIST OF ABBREVIATIONS

CSCs- Cancer Stem Cells

°C- degree centigrade

DLS- Dynamic Light Scattering

DSPE-PEG- 1,2-distearoyl-*sn*-glycero-3-phosphoethanolamine-N-[amino(polyethylene glycol)]

FTIR- Fourier Transform Infrared

LMV- large multilamellar vesicles

μM- micro molar

Psi- Pounds per square inch

SEM- Scanning Electron Microscopy

SUV- small unilamellar vesicles

**CHAPTER 1**  
**ABSTRACT**



# **Study on Curcumin based nanomedicine against cancer stem cells**

Naina Gupta

Delhi Technological University, Delhi, India

## **ABSTRACT**

Present within a tumour is a subpopulation of cells known as cancer stem cells which can renew themselves, differentiate into tumour cells and are capable of inducing tumour if transplanted into an animal host. These are responsible for drug resistance, metastasis and recurrence of cancer. Drug resistance in these cells is a combined effect of certain properties such as presence of drug efflux transporters and detoxifying enzymes, ability to repair its own DNA and over-expression of anti-apoptotic proteins. Existing chemotherapy and radiotherapy techniques fail to eradicate these cells. Controlled drug delivery by nanomaterials holds great potential to overcome this barrier as it surpasses the low aqueous solubility and stability of most anticancer drugs that are known and requires low drug dosage thereby reducing non specific toxicity by targeting specific site. Small size also increases penetration of nanomaterials inside the tumour. Nanomaterials can be liposomes, nanoparticles, nanotubes, micelles, etc. Easy to synthesize, micelles have been reported as effective drug carriers against cancerous cells. Present work proposes a potential anticancer role of the well known natural product- Curcumin which is being utilised for the treatment of various diseases and has been reported to hinder angiogenesis and tumour growth. In this study, DSPE-PEG micelles were successfully prepared by film dispersion method and loaded with Curcumin. These were then characterised for particle size, drug encapsulation efficiency and morphology. Finally, the nanoformulation was tested for its anticancer activity on YAC-1 cells. The prepared nanoformulation had an average size of 108.9nm and comprised a major population of circular shaped molecules. It was observed that treating YAC-1 cells by this nanoformulation at 20 $\mu$ M concentration for 72 hours, more than 90% of the cells died.

**CHAPTER 2**  
**INTRODUCTION**

# INTRODUCTION

Cancer stem cells (CSCs) are cancer cells which have properties similar to stem cells and are present within a tumour. CSCs are able to self renew themselves and differentiate into cells that are present in a particular type of cancer. These are responsible for drug resistance, metastasis and recurrence of cancer (Gupta et al., 2009). Drug resistance in these cells is a combined effect of certain properties such as presence of drug efflux transporters and detoxifying enzymes, ability to repair its own DNA and over-expression of anti-apoptotic proteins. Current anti-cancer therapies are based on shrinking the tumour thus killing only the bulk of cancer cells but CSCs (Scadden et al., 2006). The new tumour that reverts back again is usually resistant to the previously used therapy. Therefore, targeting the root cause of the tumour is essential. Existing chemotherapy and radiotherapy techniques fail to eradicate these cells.

Existing methods for treatment of cancer-

1. Surgery- It involves the removal of cancer from the body. Surgeon cuts and takes off the cancer tissue from the body. But this is a painful technique and needs time for recovery. Alternatively, other methods are used such as-
  - Cryosurgery- Abnormal tissue is destroyed by extreme cold produced by liquid nitrogen or argon gas. This is used to treat retinoblastoma, early stage skin cancer and precancerous growths on skin and cervix.
  - Laser- Laser is used to cut through tissue and is effective for precise surgery. It can also shrink or destroy precancerous growths and are commonly used against tumors on the body surface or inner lining of internal organs.
  - Hyperthermia- Hyperthermia uses high temperatures thereby either killing tumour cells or making them more vulnerable to chemo or radiotherapy.
  - Photodynamic therapy- It involves the use of drugs which activate when tumor is exposed to a certain type of light. It is usually used against skin cancer.
2. Radiation therapy- In radiation therapy or radiotherapy, high doses of radiation is used to kill cancer cells or to shrink tumor. This therapy reduces the tumor size if given before the surgery or kills residual cancer cells if given post surgery. It is also given to the patient during surgery so that the radiations go straight to the cancer bypassing skin. Apart from cancer cells, radiation also affects nearby healthy cells. Therefore, patients

who are treated with radiation may suffer fatigue, hair loss, skin changes and other symptoms depending upon which area of the body has been treated.

3. Chemotherapy- Chemotherapy involves the use of drugs to kill cancer cells or to ease cancer symptoms such as pain by shrinking the tumor. It is combined with other therapies for better treatment. It can be given before surgery or radiation therapy to shrink the tumor. It can also be given after surgery to kill cancer cells that remain after treatment. Apart from cancer cells, chemotherapy also kills healthy cells such as hair follicles and cells that line the mouth and intestine. Therefore chemotherapy can cause hair loss, mouth sores, fatigue and nausea (Monsuez et al., 2010; Dodd et al., 1993).
4. Immunotherapy- Immunotherapy is a type of biological therapy that boosts up body's immune system to fight against cancer. Several immunotherapies include monoclonal antibodies, T-cell therapy, cytokines and treatment vaccines. Cancer cells are known to develop markers that hide them from recognition by the immune cells. Immunotherapy can help overcoming this barrier. Some of the common side effects of immunotherapy are pain, redness, nausea, fatigue, weakness, swelling, diarrhoea, etc.
5. Hormone therapy- This therapy stops or slows the growth of cancers that use hormones to grow. It either blocks hormone production or interfere with the effect of hormone on cancer cells. It is commonly used to treat prostate and breast cancer. Tumors that are not sensitive to hormones do not have hormone receptors and thus are insensitive to this therapy. Hormone receptor positive breast cancer cells can be treated by hormone therapy by lowering the amount of estrogen in the patient's body or by blocking its action on breast cancer cells. Some of the hormonal therapy medicines are aromatase inhibitors, estrogen receptor down regulators and selective estrogen receptor modulators. Hormone therapy can cause fatigue, nausea, hot flashes, diarrhoea, mood changes and weakened bones.

One of the major challenges of drug formulation industries is the low aqueous solubility of drugs. Reports suggest that out of all the new chemical formulations developed by the pharmaceutical companies, 40% are insoluble in water. For absorption at the tumour site, the drug must be present in a solution. Various techniques are being used to increase the hydrophilicity of poorly soluble drugs such as by modifying the physiology or chemistry of the drug or by reducing the drug size, using a surfactant, co solvency, etc. (Savjani et al, 2012). Another approach is to load the drug into a carrier which is soluble in water. Nanocarriers are being widely studied for efficient drug delivery.

Controlled drug delivery by nanomaterials holds great potential against CSCs as it surpasses the low aqueous solubility and stability of most anticancer drugs and requires low drug dosage thereby reducing non specific toxicity by targeting specific site. Simultaneously, nanomaterials increase bioavailability and circulation time of the drug encapsulated. Small size also increases penetration of nanomaterials inside the tumor. A wide knowledge of nanomaterials is being applied in the field of drug designing and medicine (Torchilin et al., 2011; Prabhakar et al., 2013).

Nanomaterials can be of various types- nanoparticles, nanotubes, dendrimers, micelles, liposomes, fullerenes, nanorobots, etc. Micelles are aggregates of amphipathic molecules formed in water that have polar head groups at the exterior surface and non-polar hydrophobic tails in the interior. Hydrophobic core of micelle allows loading of lipophilic drugs that are insoluble in water. The brush-like structure of hydrophilic part protects the hydrophobic part from biological invasion. Since the size of micelles is above the threshold for renal clearance (~5nm), they are retained in the bloodstream. Micelles have good drug loading capacity and can carry many drugs with prolonged circulation times. Drug loaded nanocarriers are released into the bloodstream and accumulate into leaky vasculature sites such as tumors and sites of inflammation due to enhanced permeability and retention effect (EPR) (Zaheer Ahmed). Micelles are easy to synthesize and have been reported to successfully deliver drugs against cancer cells (Jhaveri et al., 2014; Paliwal et al., 2011).

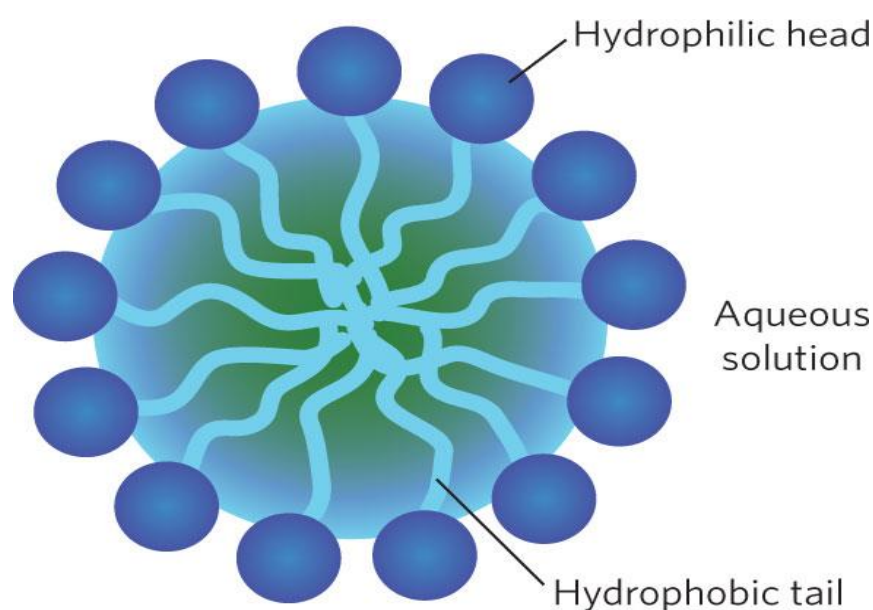


Figure 2.1: Structure of a micelle

Source- [http://www.nature.com/nmat/journal/v9/n5/fig\\_tab/nmat2761\\_F1.html](http://www.nature.com/nmat/journal/v9/n5/fig_tab/nmat2761_F1.html)

A wide number of drugs are being studied against cancer. One such potential drug is a well known natural product called Curcumin which is the principal Curcuminoid present in turmeric. It is derived from *Curcuma Longa* plant which belongs to the family Zingiberaceae. Lipophilic in nature, Curcumin is insoluble in water but readily dissolves in organic solvents such as methanol, acetone and dimethylsulfoxide. It is known to give turmeric its yellow colour and has received tremendous attention in Ayurveda for its role in anti-oxidant, analgesic, antiseptic, anti-inflammatory and antimalarial properties. Recently, it has also been reported as an anticancer drug as it affects pathways that are involved in mutagenesis, cell cycle regulation, oncogene expression, apoptosis, metastasis and tumorigenesis (Ammon et al., 1991; Aggarwal et al., 2003).

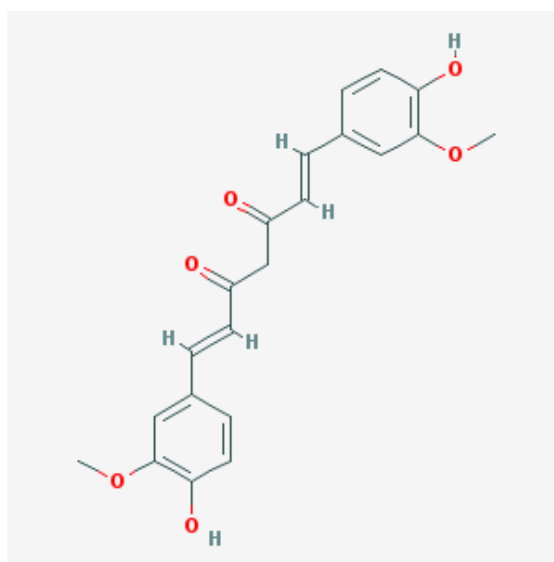


Figure 2.2: Chemical structure of Curcumin

Source- PubChem

**CHAPTER 3**  
**REVIEW OF LITERATURE**

# REVIEW OF LITERATURE

First identified in 1994 in human acute myeloid leukemia, cancer stem cells (CSCs) are present inside a tumor that are able to self renew, differentiate and induce tumor if transplanted into an animal host. Therefore, these cells are also termed as ‘tumor-initiating cells’. CSCs have been reported to be present in various percentages in different types of cancers ranging from 0.1% to 30%. CSCs possess certain intrinsic or acquired properties that make these cells resistant to drugs. Existing chemotherapies and radiotherapies kill the bulk of cancer cells but fail to eradicate these cells which give rise to recurrence of the tumor and metastasis. The new tumor formed spreads faster, becomes more malignant and resistant to the drugs that were used in the past (Gupta et al., 2009).

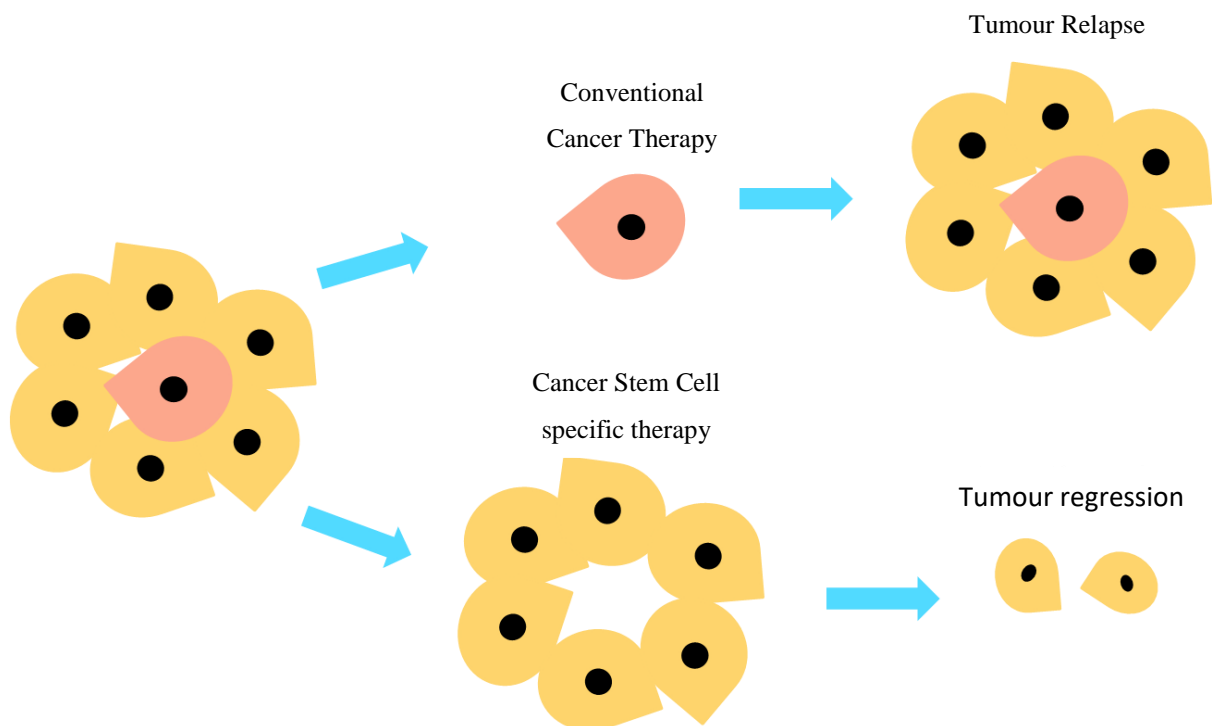


Figure 3.1: Need for Cancer Stem Cell specific therapy

CSCs are characterised by specific markers such as  $CD34^+/CD38^-$  in leukemia cells,  $CD44^+/CD24^-$  in solid tumors or  $CD133^+$  in other tumors. CD44 binds to hyaluronic acid (HA) that is present in extracellular matrix thus helping in the attachment of CSCs to the extracellular matrix and ultimately leading to metastasis. Targeting these markers can be used to deliver drugs specifically against CSCs (Scadden et al., 2006).



CSCs are known to possess drug efflux transporter proteins also known as ABC transporters for example P-glycoprotein (P-gp), breast cancer resistant protein (BCRP) and the multidrug resistance- associated proteins (MRP). P-gp is known to efflux out drugs in various therapies against solid tumors and leukemia. It has been reported that blocking ABCB5 glycoprotein by anti-ABCB5 monoclonal antibody restored the sensitivity of melanoma cells to doxorubicin (DOX). This suggests that these transporters can be potential therapeutic targets to overcome drug resistance by CSCs.

In quiescence, both SCs and CSCs self renew and maintain their population. Various genes and signalling pathways help maintaining the CSCs in tumour microenvironment. Hedgehog signalling pathway which plays an important role in embryo development, directs cell proliferation, epithelial to mesenchymal transitions, cell fate determination and rearrangement of cells by motility and adhesion changes (Teglund et al., 2010). Abberant activation of Hedgehog signalling in adult can result in initiation, growth and maintenance of cancer. Hedgehog signalling drives the phenotype of CSCs by subverted regulation of stemness determining genes. Nanog, which is a key transcription factor determining the reprogramming of somatic cells into pluripotent stem cells, is a direct transcriptional target of Hedgehog signalling pathway (Ferretti et al., 2010). The Notch pathway is another conservative signalling pathway that has been associated with self-renewal and the survival of CSCs linked to the metastasis-forming ability of CSCs (Wang et al., 2009).

CSCs reside in a dynamic supportive system called CSC niche with specific anatomic and functional features that contains a variety of cell types, cytokines and signaling pathways.

Current anti-cancer therapies are based on shrinking the tumour thus killing only the bulk of cancer cells but CSCs. Accumulation of CSCs after cancer therapy leads to relapse of the disease followed by metastasis. The new tumour that reverts back again is usually resistant to the previously used therapy. Therefore, targeting the root cause of the tumour is essential. Controlled drug delivery by nanomaterials holds great potential against CSCs as it surpasses the low aqueous solubility and stability of most anticancer drugs and requires low drug dosage thereby reducing non specific toxicity by targeting specific site. Simultaneously, nanomaterials increase bioavailability and circulation time of the drug encapsulated. Small size also increases penetration of nanomaterials inside the tumor. A wide knowledge of nanomaterials is being applied in the field of drug designing and medicine.

A few drugs have demonstrated high efficacy against CSCs. A veterinary antibiotic known as polyether ionophore salinomycin is known to kill breast cancer CSCs but is toxic to humans. It has been suggested that nanoformulations incorporating this drug may be non-toxic and efficient against CSCs (Gupta et al., 2009).

A wide range of nanomaterials are being studied upon for the development of nanomedicine. These are based on organic, lipid, inorganic, protein or synthetic polymers. Nano sized therapeutics offer some great advantages in cancer treatment.

First, nanocarriers help overcoming the poor solubility and chemical instability of most anti cancer drugs. Poor water solubility restricts the bioavailability of the drug (Williams et al., 2013). Enveloping this drug into a hydrophilic nanocarrier increases the solubility and chemical stability of the drug. For example, P13K inhibitor and radiosensitizer wortmannin were incorporated into a lipid based nanocarrier thus increasing its solubility from 4mg/L to 20mg/L (Karve et al., 2012).

Second, nanocarriers enhance pharmacokinetic profile of a drug by protecting it from excretion and biodegradation. For example, drugs that are cleaved enzymatically such as siRNA by RNAses in plasma and proteins by trypsin or pepsin in stomach can be prevented from degradation by incorporating them into nanocarriers. However, nanomedicine compounds can be constructed to improve drug penetration and to redirect chemotherapy or targeted compounds selectively to tumor cells. Fourth, nanocarriers can be designed to release their payload upon a trigger resulting in stimuli-sensitive nanomedicine therapeutics. For example, drugs whose delivery is not primarily pH-dependent, such as doxorubicin can be conjugated with a pH-sensitive nanoparticle to increase cellular drug uptake and intracellular drug release (Du et al., 2011).

Finally, targeted nanomedicine therapeutics may decrease resistance of tumors against anti-cancer drugs. Generally, specific uptake reduces the probability for unspecific, MDR/ATP efflux pump-driven elimination. Therefore, nanomedicine therapeutics may prolong the circulation time of a compound and mediate stimuli-responsive drug release as well as endocytic drug uptake. This may lead to reduced resistance of tumor cells against targeted nanocarriers (Hu et al., 2009; Huwyler et al., 2002).

Micelles are aggregates of amphipathic molecules formed in water that have polar head groups at the exterior surface and non-polar hydrophobic tails in the interior. Hydrophobic

segment of the polymer forms the core of the micelles and solubilizes the hydrophobic drug molecules. Hydrophilic segment forms the corona and provides compatibility to the micelles in the aqueous environment. The hydrophobic core can accommodate a variety of hydrophobic molecules such as therapeutics and imaging agents, thus, improving the solubility and stability in the biological system. The hydrophilic corona shields the core, and protects the loaded drugs from interactions with the blood components (Jhaveri et al., 2014).

The biocompatible polymeric corona causes reduced recognition of the micelles by reticulo-endothelial systems, thus providing long circulation of the loaded component in the blood stream. The nano-ranged size along with the long circulatory property allows polymeric micelles to eventually accumulate in any compromised tissue-vasculature sites such as tumour via a passive targeting phenomenon commonly referred to as Enhanced Permeability and Retention (EPR) effect. Unlike small molecules which go in and out from the interstitial space by diffusion, macromolecules, nanocarriers, including micelles once extravasated cannot diffuse out from the interstitial space (Torchilin et al., 2011; Prabhakar et al., 2013).

Amphiphilic block co-polymers having ligand/antibodies at the distal end of the hydrophilic block possessing strong affinity for cancer homing receptors/antigens could be inserted into the micellar assembly without disrupting micellar thermodynamic stability. The newly developed surface modified polymeric micelles are actively targeted nanocarrier system that would deliver loaded cargo more efficiently to the tumor compared to passive targeted micellar system relying only on EPR effect or passive targeting for accumulation in tumor area.(Huwyler et al., 2002; Yang et al., 2013; Sawant et al., 2014)

Therefore, advantages of polymeric micelles as drug delivery carriers in cancer therapy include their potential to solubilize the pharmaceutical components of poor aqueous solubility into the hydrophobic core, improve the pharmacokinetic properties and biodistribution, specifically target their payload to the tumor tissues by tuning their size for passive targeting via EPR effect, or by anchoring tumor targeted ligands on the micellar surface by using various amenable surface functionalization techniques. Moreover, polymeric micelles offer tunable payload release when constituted by using stimuli-sensitive block co-polymers, which disassemble under certain physiologic condition triggering disassembly of the system leading to drug release.(Leao et al., 2011; Sethuraman et al., 2006)

The most common hydrophilic block in the copolymeric structure is poly(ethylene glycol) (PEG). PEG is hydrophilic, electrically neutral, non-toxic, and flexible polymer that has

commonly been used to coat nanoparticles. PEG-coating decreases the interaction of the nanocarrier-surface with serum components, thus prolonging their circulation. Other hydrophilic block forming polymers include chitosan, poly(N-vinyl pyrrolidone) (PVP), and poly(N-isopropylacrylamide) (pNIPAAm). There are various polymer blocks utilized to form micellar core, including the class of polyethers such as poly(propylene oxide) (PPO), various polyesters such as poly(L-lactide) (PLA), poly(lactide-co-glycolic acid) (PLGA), poly( $\beta$ -aminoesters), polyamino acids such as poly(L-histidine) (pHis), poly(L-aspartic acid) (pAsp) and lipids such as dioleoyl(phosphatidylethanolamine) (DOPE), distearoyl(phosphatidylethanolamine) (DSPE). In this study, DSPE-PEG micelles have been formed.

Typical micelle formation involves following steps:

- Solubilizing powdered lipid and hydrophobic drug in a suitable organic solvent. Usually, chloroform or chloroform: methanol mixtures are used.
- The solvent is then evaporated or freeze-dried to yield a lipid film.
- The film is allowed to dry on a vacuum pump.
- Then the film is hydrated with a suitable aqueous medium such as distilled water, buffer solutions, saline, and nonelectrolytes like sugar solutions.
- Hydration of the lipid film produces large multilamellar vesicles (LMV) which are downsized to nanometer scale by sonication. Sonication produces small, unilamellar vesicles (SUV) that range in about 15-50nm.
- Usually, there are two types of sonicators- bath sonicators and probe sonicators. Although probe type sonicators deliver more input energy to the lipid suspension, it causes overheating of the sample leading to lipid degradation. Also, probe tips are known to release titanium particles into the lipid suspension which need to be separated out using centrifugation. Therefore, bath sonicators are recommended for the preparation of SUV.

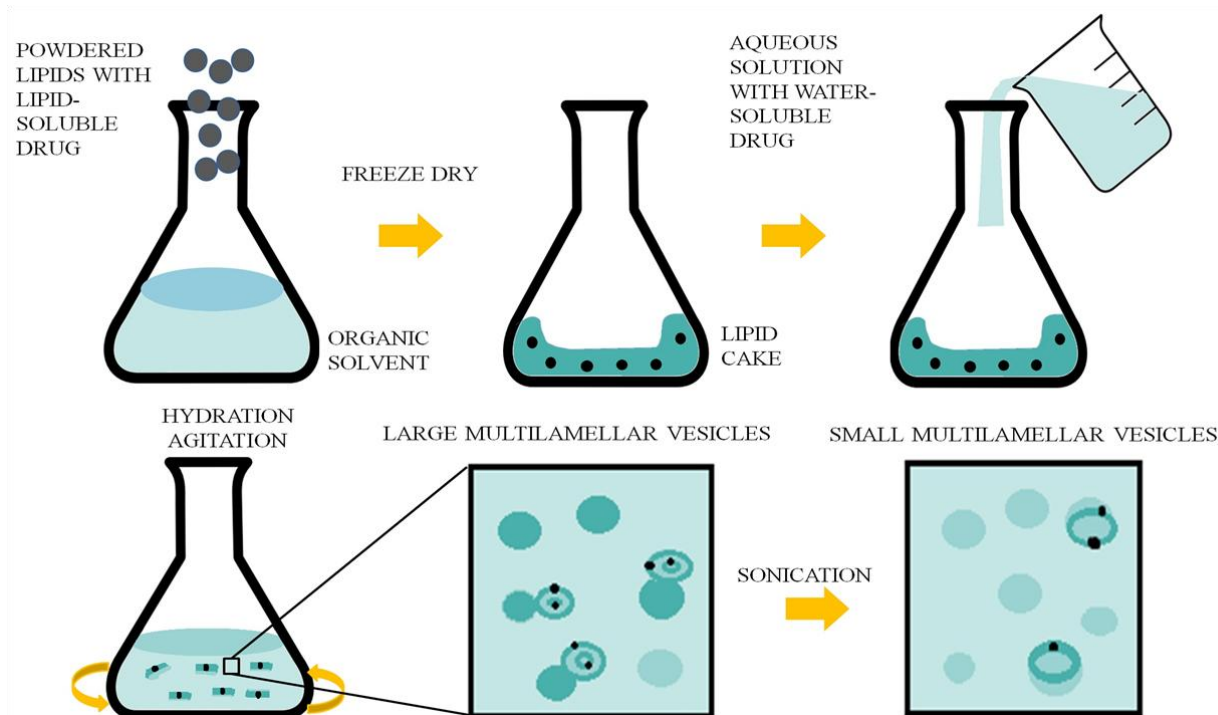


Figure 3.2: Formation of micelles

Curcumin is a polyphenol which is yellow in colour and is extracted from the rhizome of a herb *Curcuma longa* (Gandapu et al., 2011). Traditionally, it has been used as a medicine in a wide range of pharmacological actions (Shishodia et al., 2005). For years, it has been known as a potent antioxidant, anti-microbial and anti-inflammatory agent. It has also gained popularity for its anti-cancer activity over the years (Srimal & Dhawan, 1973; Sharma, 1976; Kuttan et al., 1985; Mahady et al., 2001).

A number of reports have suggested mechanisms explaining the anti cancer role of Curcumin. It can prevent the proliferation and induce apoptosis of various tumor cells (Aggarwal et al., 2003). Curcumin has been reported non-toxic for human beings (Hsu & Cheng, 2007). However, due to insolubility in water, fast elimination by the body and easy metabolism, bioavailability of Curcumin is poor. Therefore, injections and oral administration of Curcumin are not effective mediums to target the tumour (Anand et al., 2007).

Improving the stability, solubility and bioavailability of Curcumin is of great importance. One potent way to achieve this is by developing nanocarriers and incorporating Curcumin into them. The main principle in effective cancer therapy is to achieve the desired concentration of therapeutic agents at the tumour site to destroy specific cancerous cells while minimizing toxicity to normal cells (Hsu et al., 2007; Monsuez et al., 2010). It is

essential to develop Curcumin nanoformulations that exhibit better anticancer activity compared to native Curcumin.

Curcumin suppresses activation of a transcription factor, NF- $\kappa$ B that regulates expression of various genes (cyclooxygenase-2(COX-2), I $\kappa$ Ba, TNF- $\alpha$ , cyclin D1, ICAM-1, c-myc, Bcl-2, MMP-9, inducible nitric oxide synthase (iNOS), and interleukins including IL-6 and IL-8) that are involved in inflammation, cellular proliferation and cell survival (Singh et al., 1996; Brennan et al., 1998). Another transcription factor, AP-1 involved in control of cell cycle and apoptosis has been shown to be downregulated in presence of Curcumin. It has been reported that Curcumin downregulates the expression of c-jun mRNA which in turn leads to downregulation of AP-1. The c-Jun domain of AP-1 is a positive regulator of cyclin D1 expression, contributing to the induction of a tumorigenic phenotype. c-Jun is also a negative regulator of p53 expression and fibroblast cells expressing constitutive levels of c-Jun express lower levels of both p53 and the p53-regulated cyclin-dependant kinase inhibitor p21Cip1/Waf1 and fail to undergo growth arrest following UV exposure (Jobin et al., 1999; Marin et al., 2007).

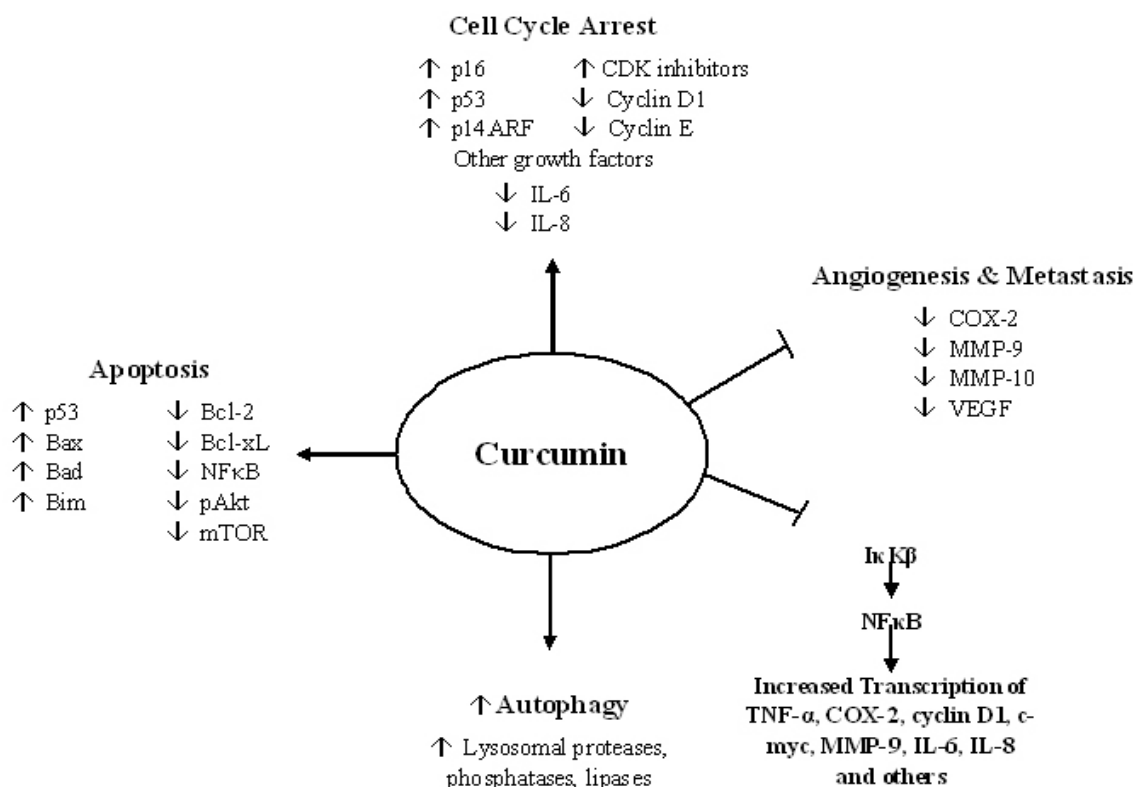


Figure 3.3: Overview of anti-cancer effects of Curcumin

Source: Wilken et al., 2012

**CHAPTER 4**  
**AIM AND OBJECTIVE**

# AIM AND OBJECTIVE

## **Aim:**

To study the *in vitro* effect of Curcumin based nanomedicine against cancer stem cells.

## **Objectives:**

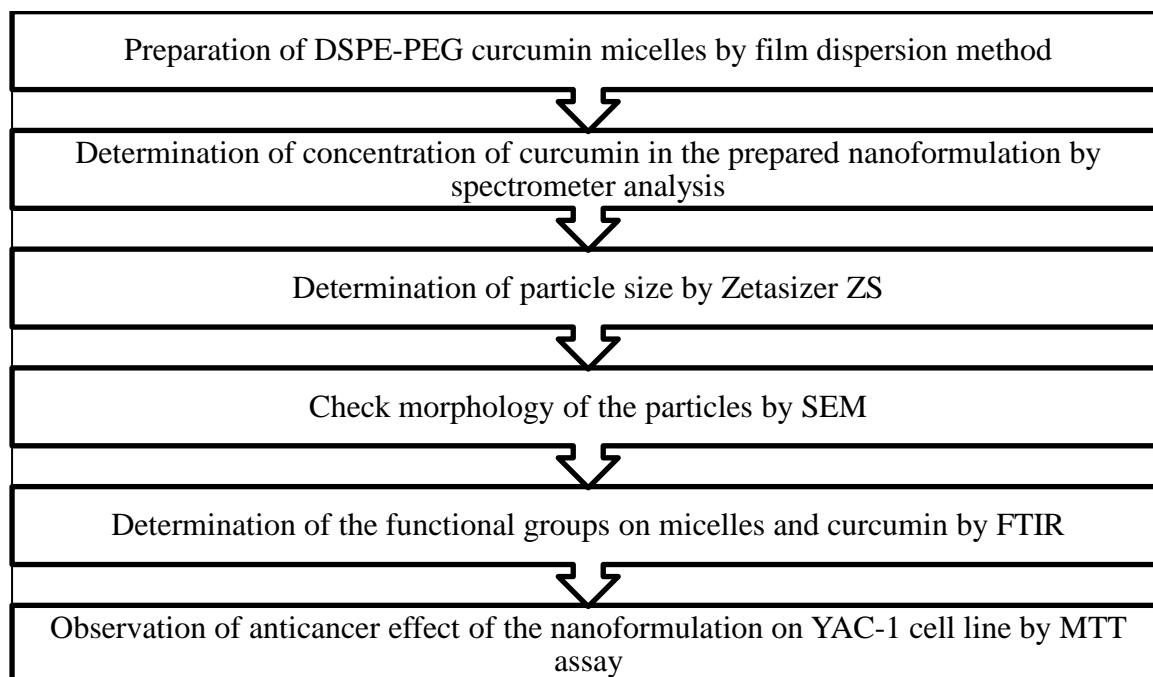
- Standardization of culture conditions of YAC-1 cell line
- Preparation of nanoformulation (micelles) incorporated with Curcumin
- Characterization of the nanoformulation
- Evaluate anticancer effect of the nanoformulation on YAC-1 cell line



**CHAPTER 5**  
**METHODOLOGY**

# METHODOLOGY

## Method Overview



YAC-1 cell line was maintained parallelly in standard culture conditions.

## Basal Media Preparation

1. Clean filter assembly was wiped with 70% ethanol.
2. 0.2 and 0.4  $\mu\text{m}$  filters were placed on their designated place onto the filter assembly.
3. Complete setup was autoclaved at 121°C, 15psi for 20 minutes.
4. The contents of RPMI-1640 were added in 1L distilled water.
5. 1.5g sodium bicarbonate was added to the solution and mixed.
6. The media was filter sterilized and stored at 4°C.

## Complete Media Preparation

1. 90mL basal media was added in a sterile 100mL bottle.
2. 10mL FBS was added to the media.

## Phosphate Buffer Saline Preparation

1. Complete filter assembly setup was autoclaved at 121°C, 15 psi for 20 minutes.
2. 137mM NaCl, 2.7 mM KCl, 10mM  $\text{Na}_2\text{HPO}_4$  and 2mM  $\text{KH}_2\text{PO}_4$  were added in 1L sterile water.
3. The solution was filter sterilized and stored at 4°C.

## **Maintenance of Cell line**

### **Subculturing**

1. Contents of a flask were transferred into two falcon tubes and centrifuged at 400g for 2 minutes.
2. Supernatant was discarded.
3. 1 ml 100X Phosphate Buffer Saline was added to each falcon tube. The pellet was gently mixed.
4. Cell count was performed using hemocytometer.
5. The falcon tubes were centrifuged at 400g for 2 minutes.
6. The supernatant was discarded and 1 mL complete media was added to each falcon tube.
7. 5ml complete media was added to a fresh T25flask
8.  $10^5$  cells were inoculated in the flask.
9. 1% antibiotic mix was added to the flask.
10. The flasks were incubated at 37°C, 5% CO<sub>2</sub>.

### **Cell viability assay**

1. Contents of a flask were transferred into two falcon tubes and centrifuged at 400g for 2 minutes.
2. Supernatant was discarded and 1 ml 100X Phosphate Buffer Saline was added to each falcon tube. The pellet was gently mixed.
3. 20µL sample was withdrawn and trypan blue was added in 1:10 ratio.
4. The resulting mix was incubated for 1 minute and visualized using hemocytometer in Phase contrast microscope.
5. The cells that appeared clear were live and the blue cells were dead.

### **Cell morphology analysis**

1. Contents of a flask were transferred into two falcon tubes and centrifuged at 400g for 2 minutes.
2. Supernatant was discarded and 1 ml 100X Phosphate Buffer Saline was added to each falcon tube. The pellet was gently mixed.
3. 20µL sample was withdrawn and Giemsa stain was added in 1:10 ratio.
4. The resulting mix was incubated for 1 minute.

5. 10 $\mu$ L was added onto a slide, covered with a coverslip and visualized using Phase contrast microscope.

### **Growth curve**

1. The number of live cells in a sample was counted using Trypan Blue and hemocytometer.
2. 10<sup>5</sup> cells/mL were inoculated in 10mL complete media in a T25 flask.
3. The flasks were incubated at 37°C, 5% CO<sub>2</sub>.
4. 100 $\mu$ L sample was withdrawn everyday and cell viability was performed using Trypan blue.

### **Formation of Curcumin micelles**

1. 20mg DSPE-PEG and 2mg Curcumin were dissolved in 1ml chloroform:methanol (3:1) in a vial.
2. Organic solvent was evaporated leaving a thin film formed at the walls of the vial.
3. The film was left for air drying for 2 hours at room temperature to ensure evaporation of residual organic solvent.
4. 1ml 100X phosphate buffer saline was added to the vial and left it for 2-3 hours for hydration of the film.
5. The solvent was transferred to a new vial.
6. Vial was then placed into an ultrasonicator (bath) for 5 minutes at room temperature.
7. Micelles were generated and stored at 4°C.

### **Characterization of Curcumin nanoformulation (micelles)**

#### **Determination of Curcumin concentration in the prepared micelles**

1. Curcumin was dissolved in methanol to prepare Curcumin solutions in five different concentrations:
2. Absorbance of Curcumin solutions was taken at 421nm using a UV-VIS spectrometer.
3. A standard curve was generated on the basis of Curcumin concentrations and their respective absorption at 421nm.
4. Absorption of drug loaded micelles was then taken at 421nm.
5. Reading of the sample was compared with the standard curve and concentration of Curcumin in the prepared nanoformulation was thus generated.

#### **Particle size characterization by DLS**

1. Prepared nanoformulation was diluted by a factor of 2.
2. It was then analysed for particle size by Zetasizer Nano ZS.

### **Morphology of nanoformulation**

- The prepared nanoformulation was then analysed by JSM-6610LV SEM instrument to check the morphology of the sample.

### **FTIR spectroscopy**

1. Both nanoformulation and Curcumin were analysed by FTIR spectroscopy to verify main functional groups in the samples.
2. They were diluted by a factor of 10.
3. FTIR spectra was generated and compared with reported spectrums of the corresponding samples.

### **Invitro anticancer activity**

1.  $10^5$  cells were seeded in 1ml media in wells of a 24 well plate.
2. Prepared Curcumin micelles were added to the media to obtain 10 $\mu$ M, 20 $\mu$ M and 40 $\mu$ M concentrations in 3 different wells, respectively. Cells in 3 wells were also treated with free Curcumin with similar concentrations. 50 $\mu$ L, 100 $\mu$ L, 150 $\mu$ L and 200 $\mu$ L volume of micelles which were free of Curcumin were also added into 4 wells, respectively. These cells and untreated cells served as controls for the experiment. The experiment was set up in duplicate for each well.
3. The plate was incubated at 37°C in 5% CO<sub>2</sub> incubator for 72 hours.
4. The cells were pelleted down and seeded into 96 wells plate with 0.18ml fresh media.
5. 20 $\mu$ L freshly prepared MTT reagent was added into each well.
6. The plate was incubated at 37°C in 5% CO<sub>2</sub> incubator for 4 hours.
7. The cells were pelleted down and 170 $\mu$ L media was removed from the wells.
8. 100 $\mu$ L DMSO was added to the wells to dissolve the violet crystals formed in the previous step.
9. Absorbance at 540nm was taken after 5 min incubation.
10. Cell viability graph was plotted.

# **CHAPTER 6**

## **RESULTS**

# RESULTS

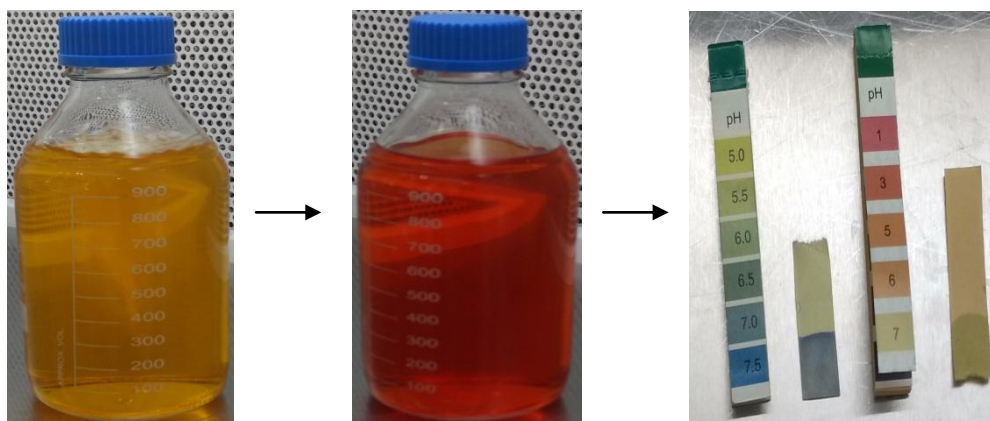
## Preparation of RPMI-1640 media

RPMI-1640 was procured from SIGMA in powder form. Figure 6.1 depicts the process of preparation of media. The media content was dissolved first in sterile water. 1.5g of sodium bicarbonate was added. pH of the media was checked by pH strips ~7. Sterile filter assembly with 0.4 $\mu$ m and 0.2 $\mu$ m filters was set up over sterile 1L bottle and media was poured into it. With the help of vacuum pump, sterile media was collected.



(a)

(b)



(c)

(d)

(e)

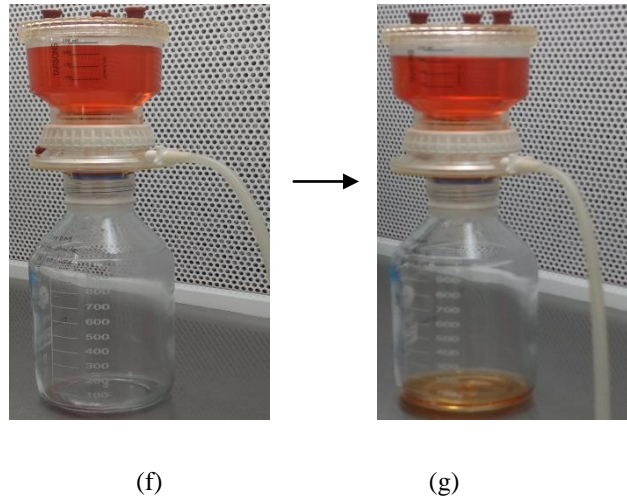


Figure 6.1: Preparation of RPMI-1640 media (a) RPMI-1640 media (b) Filtration assembly (c) Dissolution of RPMI-1640 in sterile water (d) Addition of sodium bicarbonate (e) pH of media ~7 (f) Addition of media to filtration assembly (g) RPMI-1640 media filtering into sterile 1L bottle

For complete media, 10mL FBS was added to 90mL basal media in a sterile 100mL bottle. Both basal media and complete media were stored at 4°C.

### Subculturing of YAC-1 cells

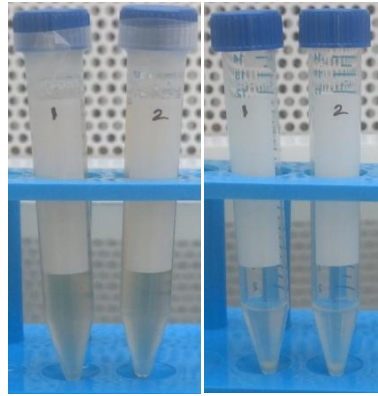
YAC-1 cell line (T cell lymphoma which was induced by inoculation of the Moloney leukemia virus (MLV) into a newborn A/Sn mouse) was procured from NCCS, Pune and maintained in the lab.

For subculturing, contents of a flask were transferred into 2 centrifuge tubes and centrifuged at 400g for 2 minutes. The media was discarded and 1mL PBS was added. After gentle mixing of the pellet, 100µL was taken out in a fresh eppendorf for cell counting. Tubes were centrifuged again at 400g for 2 minutes and PBS was discarded. 1mL media was added to both tubes and pellet was gently mixed.  $10^5$  cells were seeded into a flask containing 5mL fresh media.



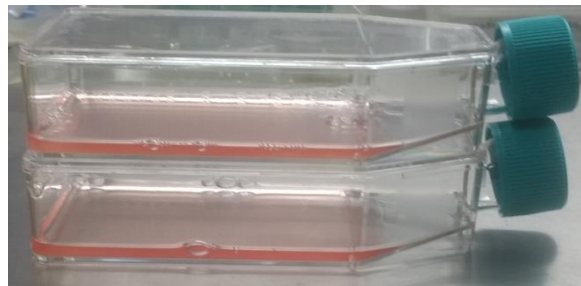
(a)  
↓





(b)

(c)



(d)

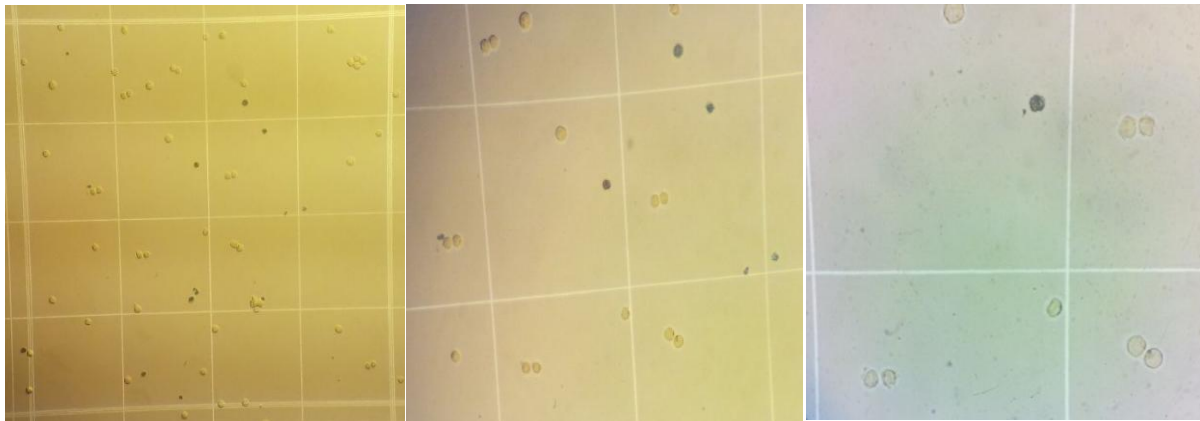
Figure 6.2: Subculturing of YAC-1 cell line: (a) T75 flasks containing  $10^7$  cells/ml, (b) Dispensing the flask contents into falcon tubes, (c) Formation of pellet following addition of PBS and centrifugation, (d) Seeding  $10^5$  cells/ml into new flasks in complete media

### YAC-1 cell viability and morphology



Figure 6.3: YAC-1 cells in T75 culture flask

Cell viability was done using hemocytometer.  $20\mu\text{L}$  PBS containing cells that was taken during subculturing was mixed with  $2\mu\text{L}$  trypan blue stain and incubated for 1 minute at room temperature.  $10\mu\text{L}$  was loaded into hemocytometer and cells were counted.



(a)

(b)

(c)

Figure 6.4: Cell viability analysis using trypan blue. Blue colored cells are dead and clear cells are live. (a) 100X Magnification (b) 200X Magnification (c) 400X Magnification

For cell morphology, 20 $\mu$ L PBS containing cells that was taken during subculturing was mixed with 2 $\mu$ L giemsa stain and incubated for 1 minute at room temperature. 10 $\mu$ L was added onto a clean slide, covered with a coverslip and observed under phase contrast microscope.

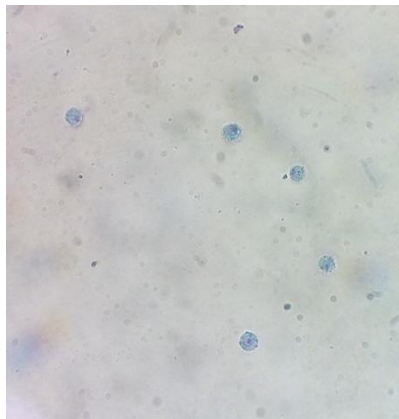


Figure 6.5: Cell morphology analysis using Giemsa stain at 400X Magnification.

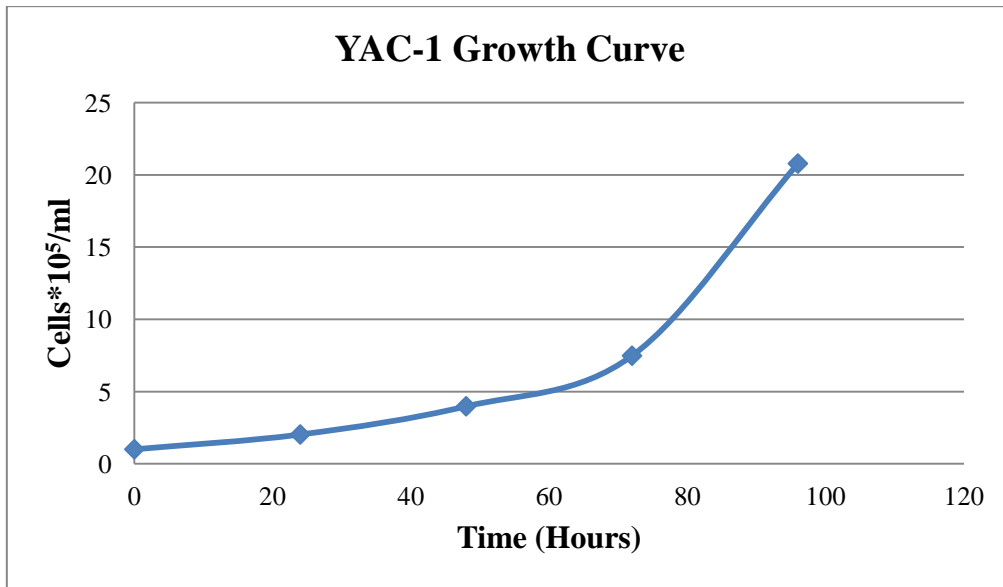
### **Growth Curve Analysis**

To obtain growth curve for YAC-1 cell line, 10<sup>5</sup> cells were seeded in a fresh flask. After every 24 hours, 100 $\mu$ L media was taken for cell counting.

Hours	Live cells/ml
0	$1 \times 10^5$
24	$2.025 \times 10^5$
48	$3.975 \times 10^5$
72	$7.475 \times 10^5$
96	$20.775 \times 10^5$

Table 6.1: Observation Table of Growth Curve Analysis

A graph representing the number of live cells per mL in the media was plotted against time.



(a)



0hr

24hr

48hr

72hr

96hr

(b)

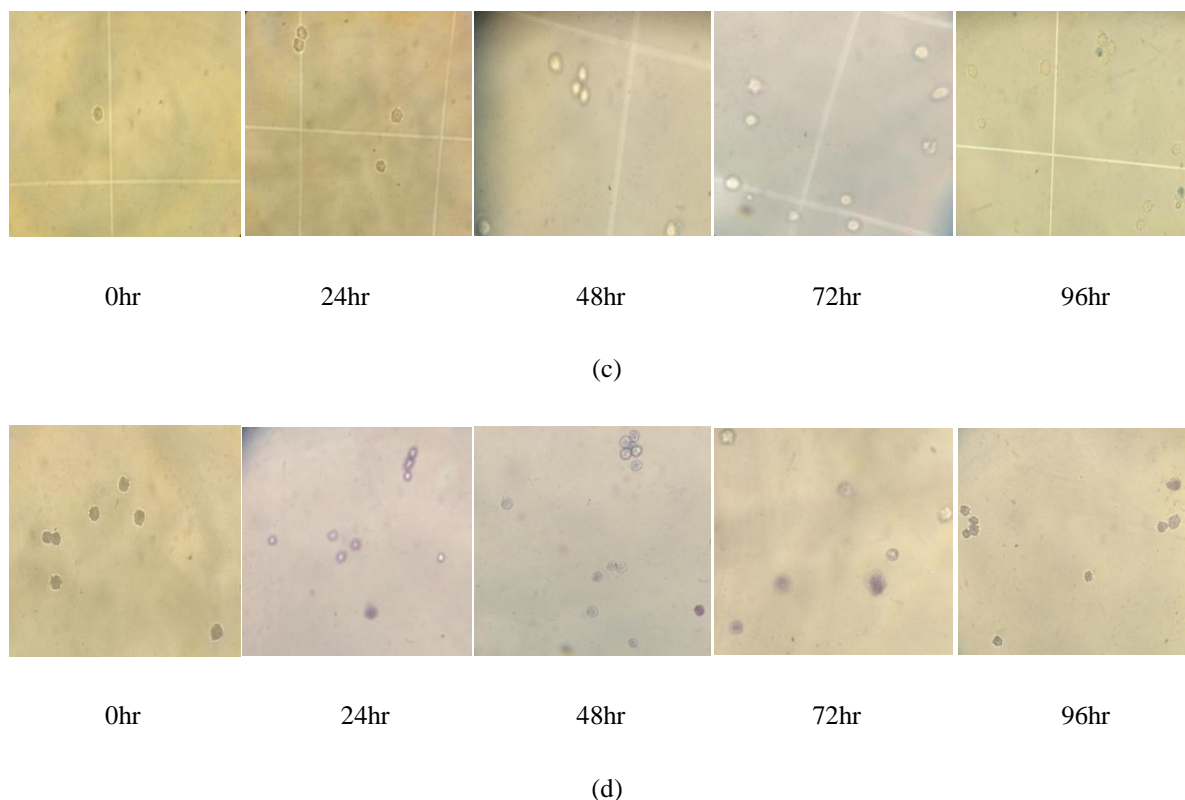


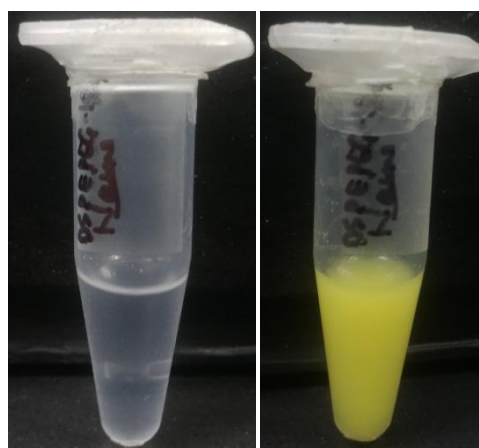
Figure 6.6: Growth curve of YAC-1 cell line – (a) graphical representation (b) cell count with hemocytometer at 100X magnification (c) cell count with hemocytometer at 400X magnification (d) cell morphology at 400X magnification

### **Formation of Curcumin micelles**

Curcumin stock was prepared by dissolving 200mg of turmeric by Golden Harvest in 40mL methanol. It was filtered by grade1 whatman filter paper to exclude out the undissolved residues.

20mg DSPE-PEG (procured from SIGMA) and 2mg Curcumin was dissolved in 1ml chloroform:methanol (3:1) in a vial to form Curcumin micelles.

For empty or unloaded micelles, 20mg DSPE-PEG was dissolved in 1ml chloroform:methanol (3:1).

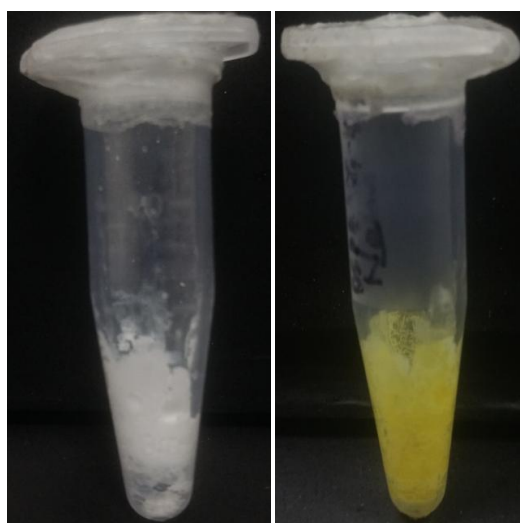


(a)

(b)

Figure 6.7: Dissolution of lipid in organic solvent (a) DSPE-PEG dissolved in chloroform-methanol (3:1) without Curcumin (b) DSPE-PEG dissolved in chloroform-methanol (3:1) with Curcumin

The organic solvent was evaporated using a heat block until a thin film was formed around the walls of the vial. It was allowed to dry at room temperature for 2 hours and then 1mL PBS was added. Film was allowed to hydrate for 3 hours and then the solvent was taken in a fresh vial for sonication.



(a)

(b)

Figure 6.8: Formation of thin film after evaporation of organic solvent while preparing (a) DSPE-PEG micelles (b) DSPE-PEG micelles loaded with Curcumin

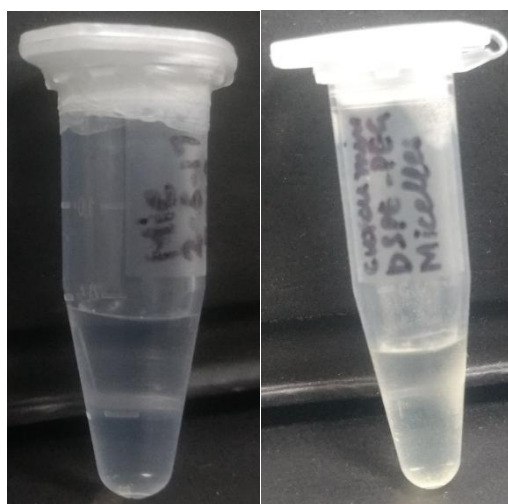
Sonication was carried out for 5 minutes at room temperature and then the vial was stored at 4°C for further analysis.



(a)

(b)

Figure 6.9: (a) Bath Sonicator (b) Sonication of Curcumin micelles for 5 minutes



(a)

(b)

Figure 6.10: Appearance of (a) DSPE-PEG micelles (b) DEPE-PEG micelles loaded with Curcumin

## Curcumin Standard Curve generation to determine concentration of Curcumin in nanoformulation

Solutions of Curcumin in methanol were prepared at different concentrations: 0.0001mg/ml, 0.001mg/ml, 0.01mg/ml, 0.1mg/ml and 0.2mg/ml. Absorbance of all the solutions was taken at 421nm using a spectrometer.

Concentration (mg/ml)	Absorbance at 421nm
0.0001	0
0.001	0.025
0.01	0.113
0.1	1.023
0.2	2.599

Table 6.2: Observation Table of Curcumin Standard Curve

A graph representing absorbance vs. concentrations of Curcumin in methanol was plotted. This was taken as a standard curve to determine the concentration of Curcumin in prepared nanoformulation.

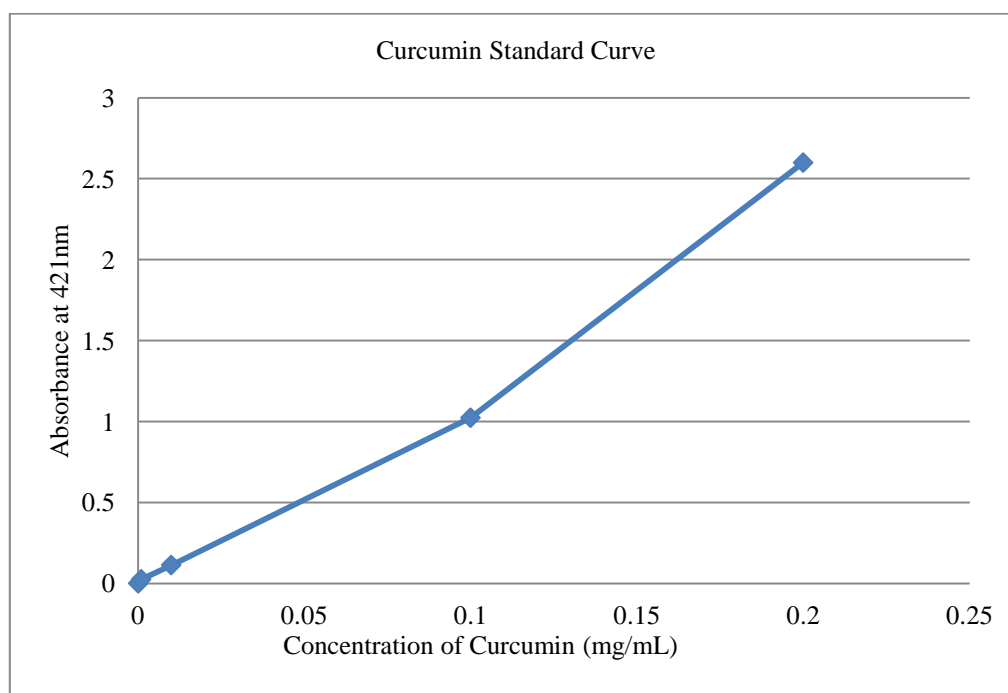


Figure 6.11: Graphical Representation of Curcumin Standard Curve

Absorbance of Curcumin in DSPE-PEG micelles loaded with Curcumin was 0.291. From above graph, concentration of Curcumin was calculated i.e. 0.026mg/ml (70.6 $\mu$ M). Absorbance of DSPE-PEG micelles that were not loaded with Curcumin was 0.

## Particle size analysis of Curcumin micelles

The prepared nanoformulation was diluted by a factor of 2 and analysed by Dynamic Light Scattering using Malvern Zetasizer Nano ZS for determination of particle size. This was carried at SMITA Labs, IIT delhi.

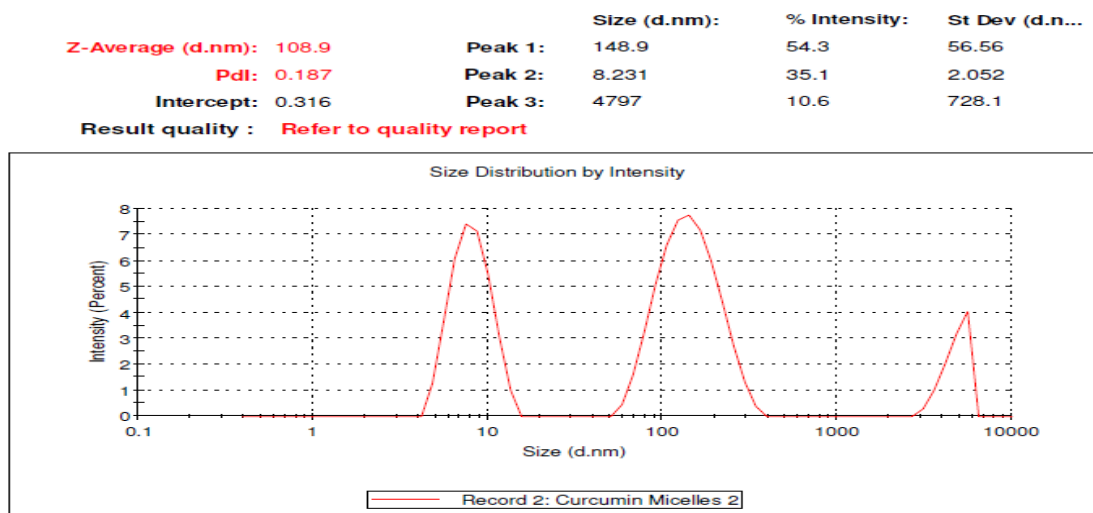


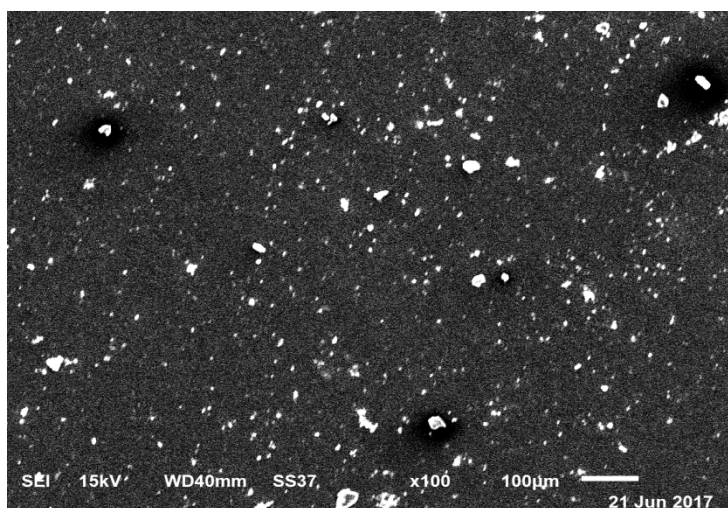
Figure 6.12: Particle size of Curcumin micelles

Average size of the nanoformulation was 108.9nm. The figure shows that the nanoformulation which was prepared was not homogenous. Possibly, there were clumps of micelles in the formulation that gave a peak of 4797nm. Therefore, it was first filtered via 0.22micron syringe filter in sterile environment and then stored at 4°C for evaluation of *in-vitro* anticancer activity.

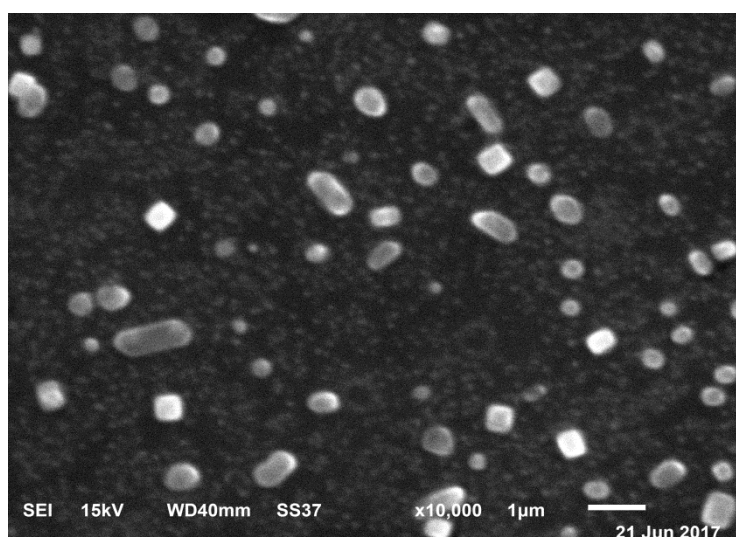
## SEM images of micelles

To determine morphology of the particles, SEM was carried out. This was done at SEM Laboratory, Department of Botany, Delhi University. Figure 6.13 illustrates that the morphology of the particles was mostly circular. Some particles being rod shaped depicts that the formulation was not exactly homogeneous.





(a)



(b)

Figure 6.13: SEM images of DSPE-PEG micelles loaded with Curcumin (a) at 100X (b) at 10kX taken from JSM-6610LV SEM instrument

### **Fourier Transform Infrared (FTIR) Spectroscopy**

An FTIR spectrum determines the main functional group of a molecule. It was carried out to know the functional groups of the drug and lipid used. Sample was diluted by a factor of 10 and analysed by FTIR spectroscopy.

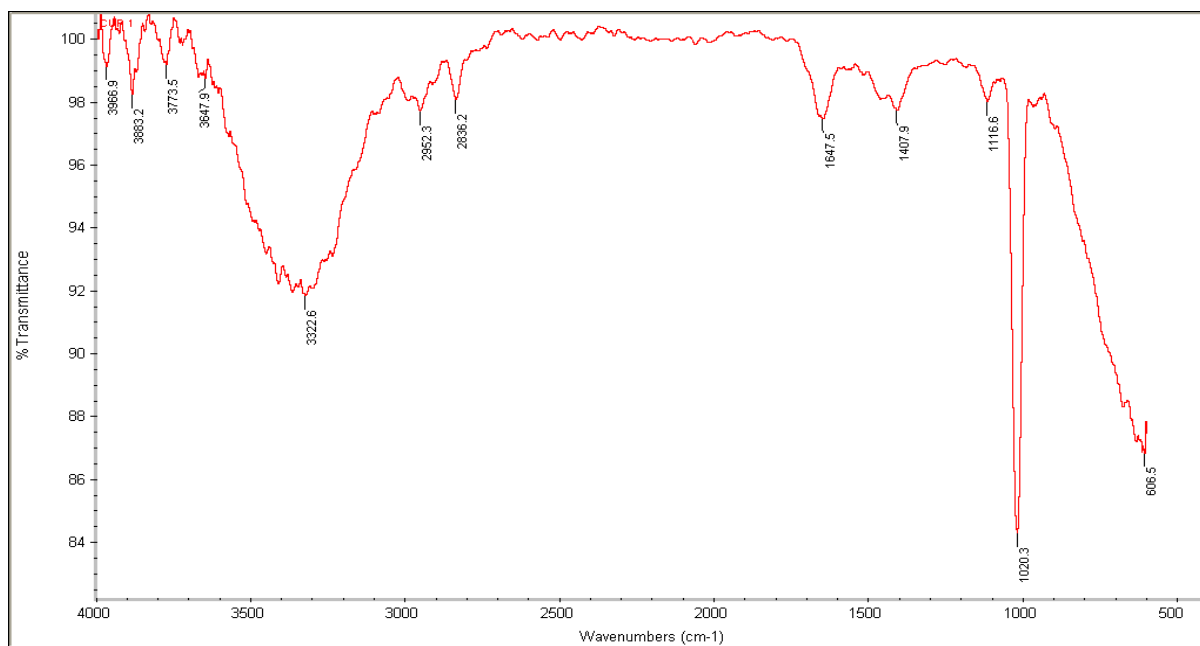


Figure 6.14: FTIR spectrum of Curcumin

- A broad peak at  $3322\text{ cm}^{-1}$  and sharp peak at  $3647\text{ cm}^{-1}$  indicate the presence of OH
- A strong peak at  $1647\text{ cm}^{-1}$  indicates presence of symmetric aromatic ring stretching vibrations ( $\text{C-C}_{\text{ring}}$ )
- The peaks at  $1407\text{ cm}^{-1}$  and  $1020\text{ cm}^{-1}$  are assigned to  $\nu(\text{C=O})$  and C-O-C, respectively

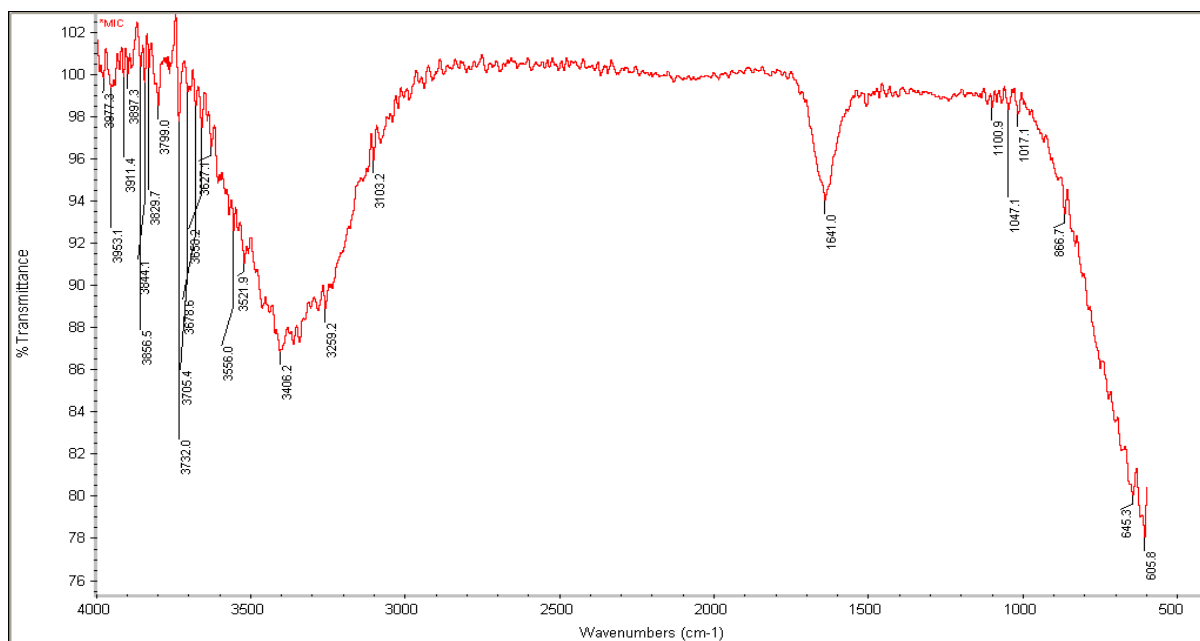


Figure 6.15: FTIR spectrum of Curcumin micelles

- The FTIR spectra showed a characteristic band representing carbonyl ketone at  $1,641\text{ cm}^{-1}$
- CH alkyl stretching band was found at  $3103\text{ cm}^{-1}$

### **Evaluation of anti cancer activity on YAC-1 cells**

For evaluation of anti cancer activity, the nanoformulation was tested on YAC-1 cell line. Three concentrations of Curcumin in nanoformulation were tested-  $10\mu\text{M}$ ,  $20\mu\text{M}$  and  $40\mu\text{M}$ . At same concentrations, free Curcumin was also added to the cells to check whether the nanoformulation is effective over free Curcumin or not. Unloaded micelles in different volumes were added to cells to determine if the lipid itself is toxic to the cells. Controls were also placed to know that the cells were growing normally given the same set of parameters.

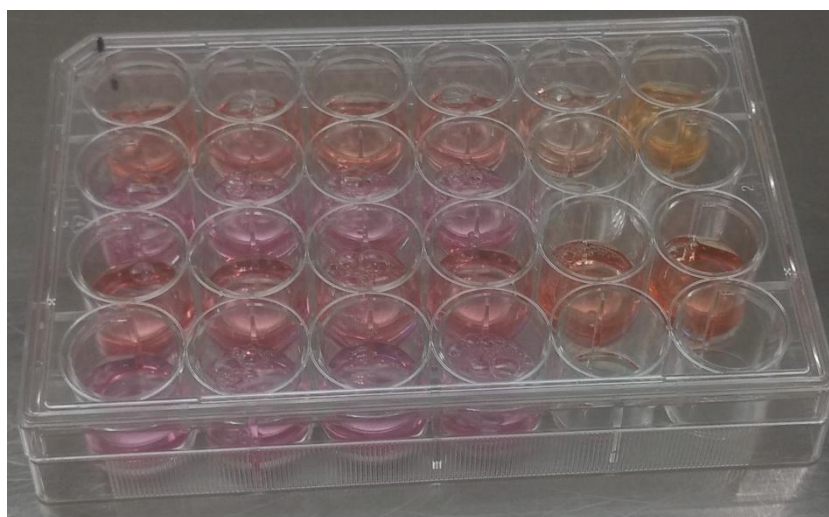


Figure 6.16: Evaluation of anticancer activity in 24 wells plate. Lane 1 has Curcumin micelles with following concentrations:  $10\mu\text{M}$   $10\mu\text{M}$   $20\mu\text{M}$   $20\mu\text{M}$   $40\mu\text{M}$   $40\mu\text{M}$ . Lane 2 has micelles without Curcumin with following volumes:  $50\mu\text{L}$   $100\mu\text{L}$   $150\mu\text{L}$   $200\mu\text{L}$ . Lane 3 has free Curcumin with following concentrations:  $10\mu\text{M}$   $10\mu\text{M}$   $20\mu\text{M}$   $20\mu\text{M}$   $40\mu\text{M}$   $40\mu\text{M}$ . Wells in lane 4 are controls (only media).

Figure 6.17 depicts the image of 24 wells plate after 72 hours of incubation in 5%  $\text{CO}_2$  incubator.

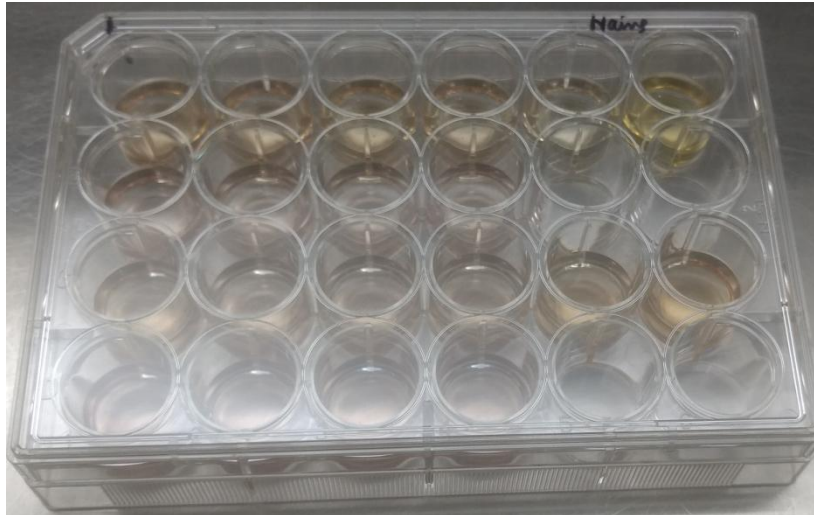


Figure 6.17: 24 wells plate after 72 hour incubation in 5% CO<sub>2</sub> incubator.

After 72 hours, cells were pelleted down and seeded into 96 wells plate with 0.18mL fresh media. 20 $\mu$ L MTT reagent was added to all wells. The plate was incubated for 4 hours in a 5% CO<sub>2</sub> incubator until violet coloured precipitates were visible in the wells.

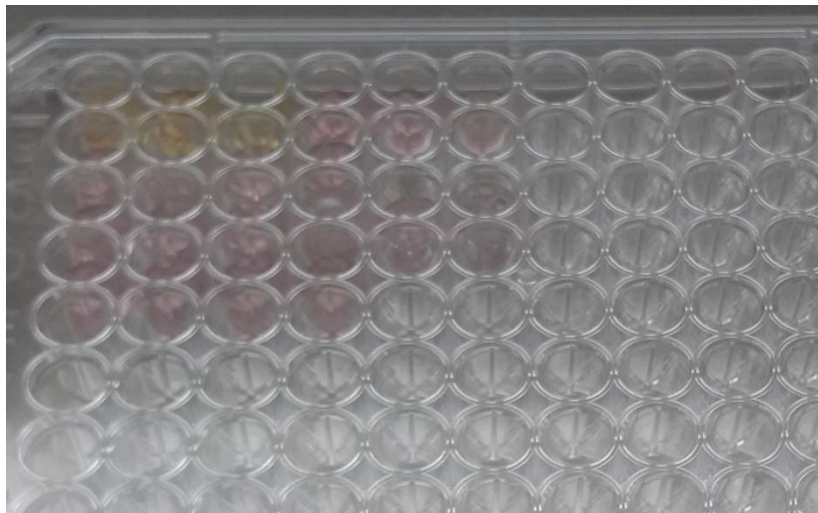


Figure 6.18: Cells plated into 96 wells plate for MTT assay

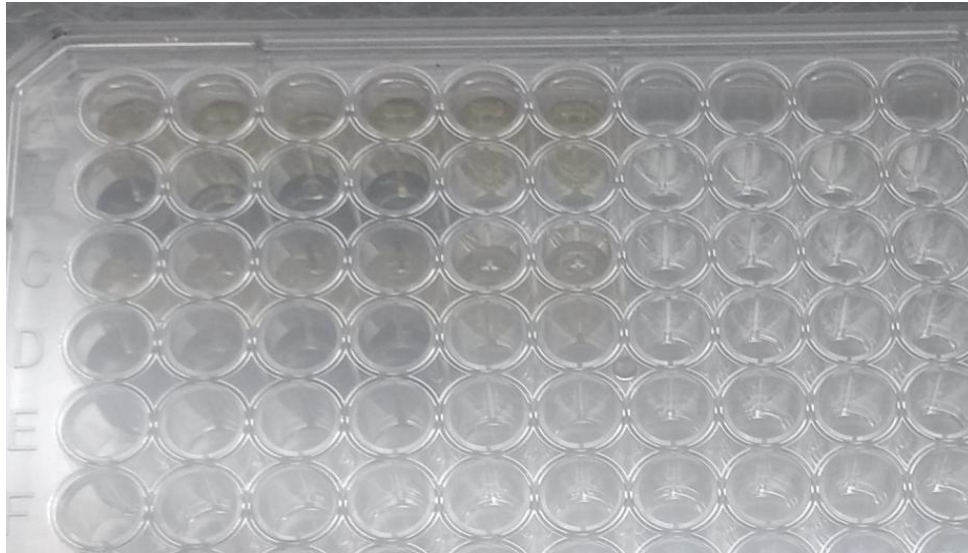


Figure 6.19: Cells treated with MTT assay after 4 hours of incubation in 5% CO<sub>2</sub> incubator

The cells were again pelleted down and approximately 170µL media was discarded from all wells. 100µL DMSO was added to solubilise formazon crystals and absorbance was taken at 540nm after 5 minutes of incubation.

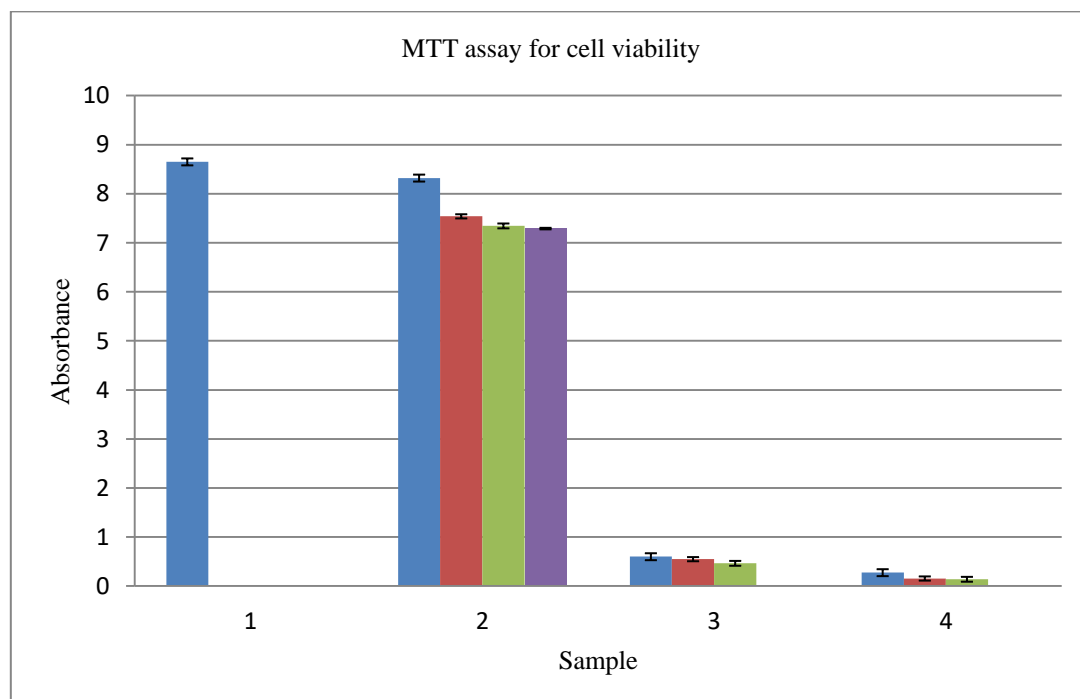


Figure 6.20: Graph representing cell viability by MTT assay. Columns in different Group represent the following: 1: Control. 2: Cells treated with unloaded micelles in following volumes: 50µL, 100µL, 150µL and 200µL. 3: Cells treated with free Curcumin in following concentrations: 10µM, 20µM and 40µM. 4: Cells treated with Curcumin micelles in following concentrations: 10µM, 20µM and 40µM.

The results indicate that unloaded micelles did not significantly lead to death of cells. Free Curcumin and Curcumin micelles show a drastic response to the cancer cells. Both Curcumin micelles and free curcumin show a drastic effect on the cells. There is approximately 5% less cell viability in case of cells that were treated with Curcumin micelles than cells treated with free Curcumin.

**CHAPTER 7**  
**DISCUSSION**

## DISCUSSION

Most of the anti cancer drugs have poor solubility and stability in the biological environment. A number of reports suggest the use of nanocarriers to overcome these barriers. Small size of nanomaterials also increases their probability to reach the tumour site. Well known natural product, Curcumin is reported for its anti cancer activity. Therefore, it was chosen as the potent anti cancer drug for the study. There are various types of biomaterials which can be used for making different types of nanoparticles depending upon the suitability, availability and feasibility of the overall experimental/therapeutic settings. One of them is micelles which are easy to synthesise and have been reported as effective drug carriers against cancer. In this study, DSPE-PEG micelles were prepared by film dispersion method and Curcumin was loaded into them. Scanning electron microscopy showed that the morphology of micelles was mostly circular with a few rod shaped molecules. Particle size analysis suggested that the average size of the prepared nanoformulation was 108.9nm. A few molecules that produced a peak at 4797nm were probably clusters of micelles. These were eliminated by filtering the formulation by 0.2µm filter. Major functional groups of the micelle and Curcumin were confirmed by FTIR spectroscopy. With the help of spectrometer, concentration of Curcumin that was incorporated into micelles was calculated. These micelles were then evaluated for their anti cancer activity. Unloaded micelles were also tested to check if the micelle itself was toxic to the cells. Cell viability was tested by Curcumin as well as Curcumin in nanoformulation. It was observed that unloaded micelles did not kill cells significantly implying that they were non-toxic to the cells. Free Curcumin killed approximately 5% fewer cells at same concentrations than Curcumin bound to micelles. The concentrations of Curcumin taken in this study showed a significant response against cancer cells and killed almost all cells in the media in 72 hours. It is suggested that a further study needs to be done which aims to identify concentrations of Curcumin micelles and free Curcumin that can kill 40-50% of cancer cells. It may provide better understanding in the effectiveness of Curcumin used as nanocarrier over free Curcumin.



**CHAPTER 8**  
**CONCLUSION**

## CONCLUSION

Curcumin micelles were successfully prepared by film dispersion method. They were found to be circular in shape and with an average size of 108.9nm. Parellely, YAC-1 cell line was maintained at standard culture conditions. The *in vitro* studies suggested that unloaded micelles were not toxic to the cells. On the other hand, Curcumin micelles and free Curcumin had significant effect on the viability of cancer cells. Free Curcumin killed ~5% less cells than Curcumin as a nanoformulation. A further analysis needs to be done by varying concentrations of Curcumin micelles and free Curcumin such that only 40-50% of the cells are killed. This would enhance our knowledge on how effective the drug is when used as a nanocarrier rather than in its native form.

**CHAPTER 8**  
**REFERENCES**

## REFERENCES

1. Teglund S., Toftgård R. Hedgehog beyond medulloblastoma and basal cell carcinoma. *Biochim. Biophys. Acta (BBA)—Rev. Cancer.* 2010;1805:181–208. doi: 10.1016/j.bbcan.2010.01.003.
2. Po A., Ferretti E., Miele E., De Smaele E., Paganelli A., Canettieri G., Coni S., di Marcotullio L., Biffoni M., Massimi L., et al. Hedgehog controls neural stem cells through p53-independent regulation of Nanog. *EMBO J.* 2010;29:2646–2658. doi: 10.1038/emboj.2010.131.
3. Wang Z, Li Y, Kong D, et al. Acquisition of epithelial–mesenchymal transition phenotype of gemcitabine-resistant pancreatic cancer cells is linked with activation of the notch signalling pathway. *Cancer Res.* 2009; 69(6):2400–2407. [PubMed: 19276344]
4. Scadden DT., The stem-cell niche as an entity of action. *Nature.* 2006; 441(7097):1075–1079.
5. Gupta PB, Onder TT, Jiang G, et al. Identification of selective inhibitors of cancer stem cells by high-throughput screening. *Cell.* 2009; 138(4):645–659. [PubMed: 19682730]
6. H.D. Williams, N.L. Trevaskis, S.A. Charman, R.M. Shanker, W.N. Charman, C.W. Pouton, et al., Strategies to address low drug solubility in discovery and development, *Pharmacol. Rev.* 65 (2013) 315–499.
7. S. Karve, M.E. Werner, R. Sukumar, N.D. Cummings, J.A. Copp, E.C. Wang, et al., Revival of the abandoned therapeutic wortmannin by nanoparticle drug delivery, *Proc. Natl. Acad. Sci. U. S. A.* 109 (2012) 8230–8235. doi:10.1073/pnas.1120508109.
8. J.-Z. Du, X.-J. Du, C.-Q. Mao, J. Wang, Tailor-made dual pH-sensitive polymer-doxorubicin nanoparticles for efficient anticancer drug delivery, *J. Am. Chem. Soc.* 133 (2011) 17560–17563. doi:10.1021/ja207150n.
9. C.-M.J. Hu, L. Zhang, Therapeutic nanoparticles to combat cancer drug resistance, *Curr. Drug Metab.* 10 (2009) 836–841.
10. J. Huwyler, A. Cerletti, G. Fricker, A.N. Eberle, J. Drewe, By-passing of P-glycoprotein using immunoliposomes, *J. Drug Target.* 10 (2002) 73–79. doi:10.1080/10611860290007559.

11. Yang C, Zhao H, Yuan H, Yu R, Lan M. Preparation and characterization of thermosensitive and folate functionalized Pluronic micelles. *J Nanosci Nanotechnol*. 2013 Oct;13(10):6553-9.
12. Sawant RR, Jhaveri AM, Koshkaryev A, Zhu L, Qureshi F, Torchilin VP. Targeted transferrin-modified polymeric micelles: enhanced efficacy in vitro and in vivo in ovarian carcinoma. *Mol Pharm*. 2014 Feb 3;11(2):375-81.
13. Chung EJ, Cheng Y, Morshed R, Nord K, Han Y, Wegscheid ML, et al. Fibrin-binding, peptide amphiphile micelles for targeting glioblastoma. *Biomaterials*. 2014 Jan;35(4):1249-56.
14. Liao C, Sun Q, Liang B, Shen J, Shuai X. Targeting EGFR-overexpressing tumor cells using Cetuximab-immunomicelles loaded with doxorubicin and superparamagnetic iron oxide. *Eur J Radiol*. 2011 Dec;80(3):699-705.
15. Na K, Sethuraman VT, Bae YH. Stimuli-sensitive polymeric micelles as anticancer drug carriers. *Anticancer Agents Med Chem*. 2006 Nov;6(6):525-35.
16. Torchilin V. Multifunctional and stimuli-sensitive pharmaceutical nanocarriers. *Eur J Pharm Biopharm*. 2009 Mar;71(3):431-44.
17. Gandapu U, Chaitanya RK, Kishore G, et al. (2011). Curcumin-loaded apotransferrin nanoparticles provide efficient cellular uptake and effectively inhibit HIV-1 replication in vitro. *PloS one* 6:e23388.
18. Shishodia S, Sethi G, Aggarwal BB. (2005). Curcumin: getting back to the roots. *Ann N Y Acad Sci* 1056:206–17.
19. Srimal RC, Dhawan BN. (1973). Pharmacology of diferuloyl methane (curcumin), a non-steroidal anti-inflammatory agent\*. *J Pharm Pharmacol* 25:447–52.
20. Sharma OP. (1976). Antioxidant activity of curcumin and related compounds. *Biochem Pharmacol* 25:1811–12.
21. Kuttan R, Bhanumathy P, Nirmala K, George MC. (1985). Potential anticancer activity of turmeric (*Curcuma longa*). *Cancer Lett* 29:197–202.
22. Mahady GB, Pendland SL, Yun G, Lu ZZ. (2001). Turmeric (*Curcuma longa*) and curcumin inhibit the growth of *Helicobacter pylori*, a group 1 carcinogen. *Anticancer Res* 22:4179–81.
23. Aggarwal BB, Kumar A, Bharti AC. (2003). Anticancer potential of curcumin: preclinical and clinical studies. *Anticancer Res* 23:363–98.
24. Anand P, Kunnumakkara AB, Newman RA, Aggarwal BB. (2007). Bioavailability of curcumin: problems and promises. *Mol Pharm* 4:807–18.

25. Hsu CH, Cheng AL. (2007). Clinical studies with curcumin. *Adv Exp Med Biol* 595:471–80.
26. Monsuez JJ, Charniot JC, Vignat N, Artigou JY. Cardiac side-effects of cancer chemotherapy. *Int J Cardiol.* 2010; 144:3–15. [PubMed: 20399520]
27. Dodd MJ. Side effects of cancer chemotherapy. *Annu Rev Nurs Res.* 1993; 11:77–103. [PubMed:8217338]
28. Chan MM: Inhibition of tumor necrosis factor by curcumin, a phytochemical. *Biochem Pharmacol* 1995, 49:1551-1556.
29. Singh S, Aggarwal BB: Activation of transcription factor NF-kB is suppressed by curcumin (diferuloylmethane). *J Biol Chem* 1995, 270:24995-25000.
30. Brennan P, O'Neill LA: Inhibition of nuclear factor kappaB by direct modification in whole cells: Mechanism of action of nordihydroguaiaritic acid, curcumin and thiol modifiers. *Biochem Pharmacol* 1998, 55:965-973.
31. Jobin C, Bradham CA, Russo MP, Juma B, Narula AS, Brenner DA, Sartor RB: Curcumin blocks cytokine-mediated NF-kappa B activation and proinflammatory gene expression by inhibiting inhibitory factor I-kappa B kinase activity. *J Immunol* 1999, 163:3474-3483.
32. Marin YE, Wall BA, Wang S, Namkoong J, Martino JJ, Suh J, Lee HJ, Rabson AB, Yang CS, Chen S, Ryu JH: Curcumin downregulates the constitutive activity of NF-kappaB and induces apoptosis in novel mouse melanoma cells. *Melanoma Res* 2007, 17:274-283.
33. Bachmeier BE, Mohrenz IV, Mirisola V, Schleicher E, Romeo F, Höhneke C, Jochum M, Nerlich AG, Pfeffer U: Curcumin downregulates the inflammatory cytokines CXCL1 and -2 in breast cancer cells via NFkappaB. *Carcinogenesis* 2008, 29:779-789.
34. Hsu TC, Young MR, Cmarik J, Colburn NH: Activator protein 1 (AP-1) and nuclear factor kappaB (NF-kappaB) dependent transcriptional events in carcinogenesis. *Free Radic Biol Med* 2000, 28:1338-1348.
35. Shaulian E, Karin M: AP-1 in cell proliferation and survival. *Oncogene* 2001, 20:2390-2400.
36. Passequé E, Wagner EF: JunB suppresses cell proliferation by transcriptional activation of p16(INK4a) expression. *EMBO J* 2000, 19:2969-2679.
37. Chattopadhyay I, Biswas K, Bandyopadhyay U, Banerjee RK: Turmeric and curcumin Biological actions and medicinal applications. *Curr Sci* 2004, 87:44-50.

38. Aggarwal BB, Sundaram C, Malani N, Ichikawa H: Curcumin: The Indian solid gold. *Adv Exp Med Biol* 2007, 595:1-75.
39. Ammon HP, Wahl MA: Pharmacology of *Curcuma longa*. *Planta Med* 1991,57:1-7.
40. Aggarwal BB, Kumar A, Bharti AC: Anticancer potential of curcumin: preclinical and clinical studies. *Anticancer Res* 2003, 23:363-398.
41. Shigeta J, Katayama K, Mitsuhashi J, et al. BCRP/ABCG2 confers anticancer drug resistance without covalent dimerization. *Cancer Sci.* 2010; 101(8):1813–1821. [PubMed: 20518788]
42. Hu C, Li H, Li J, et al. Analysis of ABCG2 expression and side population identifies intrinsic drug efflux in the HCC cell line MHCC-97L and its modulation by Akt signaling. *Carcinogenesis.* 2008; 29(12):2289–2297. [PubMed: 18820285]
43. Shuai X, Ai H, Nasongkla N, Kim S, Gao J. Micellar carriers based on block copolymers of poly ( $\epsilon$ -caprolactone) and poly (ethylene glycol) for doxorubicin delivery. *Journal of Controlled Release.* 2004;98(3):415-26. 62.
44. Gaucher G, Dufresne M-H, Sant VP, Kang N, Maysinger D, Leroux J-C. Block copolymer micelles: preparation, characterization and application in drug delivery. *Journal of Controlled Release.* 2005;109(1):169-88. 63.
45. Cuong N-V, Jiang J-L, Li Y-L, Chen J-R, Jwo S-C, Hsieh M-F. Doxorubicin-loaded PEG-PCL-PEG micelle using xenograft model of nude mice: Effect of multiple administration of micelle on the suppression of human breast cancer. *Cancers.* 2010;3(1):61-78.
46. Aliabadi HM, Lavasanifar A. Polymeric micelles for drug delivery. *Expert Opin Drug Deliv.* 2006 Jan;3(1):139-62
47. Torchilin V. Tumor delivery of macromolecular drugs based on the EPR effect. *Advanced drug delivery reviews.* 2011;63(3):131-5.
48. Iyer AK, Khaled G, Fang J, Maeda H. Exploiting the enhanced permeability and retention effect for tumor targeting. *Drug discovery today.* 2006;11(17):812-8. 9.
49. Jhaveri AM, Torchilin VP. Multifunctional polymeric micelles for delivery of drugs and siRNA. *Frontiers in Pharmacology.* 2014;5:77.
50. Na K, Sethuraman VT, Bae YH. Stimuli-sensitive polymeric micelles as anticancer drug carriers. *Anticancer Agents Med Chem.* 2006 Nov;6(6):525-35.
51. U. Prabhakar, H. Maeda, R.K. Jain, E.M. Sevick-Muraca, W. Zamboni, O.C. Farokhzad, et al., Challenges and key considerations of the enhanced permeability and

- retention effect for nanomedicine drug delivery in oncology, *Cancer Res.* 73 (2013) 2412–2417. doi:10.1158/0008-5472.CAN-12-4561.
52. Paliwal, S. R., Paliwal, R., Agrawal, G. P., & Vyas, S. P. Liposomal nanomedicine for breast cancer therapy. *Nanomedicine.* 6 (6), 1085-1100(2011).
53. Mahapatro, A., & Singh, D. K. Biodegradable nanoparticles are excellent vehicle for site directed *in vivo* delivery of drugs and vaccines. *J Nanobiotechnology.* 9 (55) (2011).
54. Danquah, M., Li, F., Duke, C. B., 3rd, Miller, D. D., & Mahato, R. I. Micellar delivery of bicalutamide and embelin for treating prostate cancer. *Pharm Res.* 26 (9), 2081-2092 (2009).
55. Li, F., Danquah, M., & Mahato, R. I. Synthesis and characterization of amphiphilic lipopolymers for micellar drug delivery. *Biomacromolecules.* 11 (10), 2610-2620 (2010).
56. Halsted WS, Young HH, Clark JG. Early contributions to the surgery of cancer. *Johns Hopkins Med J* 1974;135:399–417. [PubMed: 4613916]